

A modeling investigation of the breaking wave roller with application to cross-shore currents

William R. Dally and Cheryl A. Brown¹

Ocean Engineering Program, Florida Institute of Technology, Melbourne

Abstract. A mathematical model is developed for the creation and evolution of the aerated region, or “roller,” that appears as a wave breaks and passes through the surf zone. The model, which calculates the roller’s cross-sectional area, is based on a short-wave averaged energy balance. The vertically integrated energy flux is split between the turbulent motion in the roller and the underlying organized wave motion, and the dissipation of energy is assumed to take place in the shear layer that exists at the interface between the two flow regimes. Calibration of the roller model is done by numerically solving equations for the cross-shore balances of mass and momentum, with roller contributions included, and then optimizing predictions of depth-averaged cross-shore currents. The laboratory data of *Hansen and Svendsen* [1984] for setup and cross-shore currents, driven by regular waves breaking on a planar beach, are used to set the roller model’s fitting coefficient. The model is then validated utilizing five additional laboratory data sets found in the literature. Results indicate that employing stream function theory in calculating integral properties for the organized wave motion (wave celerity, and mass, momentum, and energy fluxes) significantly improves agreement as compared to results generated using linear wave theory. Using the roller model and stream function theory, root-mean-square error for the mean current is typically 19%. The bed stress is found to play a negligible role in the cross-shore mean momentum balance, relative to the radiation stress, setup, roller momentum flux, and convective acceleration of the current.

Introduction

Although the process of wave breaking is arguably the most important phenomenon in the nearshore, little is known about the creation and evolution of the region of aerated white water, or “roller,” that appears as a wave makes the transition from nonbreaking to a fully broken state. The dominance of the roller in dissipating energy in the surf zone is self-evident, and as noted by *Svendsen* [1984a], its contributions to the mean balances of mass and momentum should also be significant. Even so, there is an understandable lack of suitable measurements of the size, shape, and internal flow properties of the roller as a function of position in the surf zone. Consequently, the few roller models that have been developed [e.g., *Svendsen*, 1984b; *Deigaard et al.*, 1991] have been tested by incorporating them into models for the mean setup and cross-shore currents, for which data are available for comparison.

For the two-dimensional, cross-shore problem, the earliest quantitative models for combined setup and cross-shore currents [*Dally*, 1980; *Borekci*, 1982] ignored the roller. Later investigations [*Svendsen*, 1984b; *Stive and Wind*, 1986; *Deigaard et al.*, 1991] included roller terms in the mass and momentum balances, but did not rigorously model the evolution of the roller itself, and required case-specific measurements of local wave and/or water level parameters as input. These early models for the mean balances of mass and momentum focused on

the vertical structure of the undertow and provided acceptable results in the inner surf zone. However, major difficulties were encountered in the “transition region” [*Svendsen*, 1984a], where breaking is initiated and the roller is created. Although decay in wave height begins at the breakpoint, laboratory observation shows clearly that setup does not begin until well inside the breakpoint [*Bowen et al.*, 1968] and also that the undertow reaches its peak strength at a notable distance landward of incipient breaking [*Nadaoka and Kondoh*, 1982].

The existence of the transition region was first indicated by *Bowen et al.* [1968] in a laboratory study of set-down and setup due to regular waves, in which they noted a distinct landward shift from the point of incipient breaking to the point where setup began. To produce this shift, which is also evident for random waves [*Battjes and Janssen*, 1978], the concept of a lag between the production of turbulent kinetic energy (TKE) due to breaking and the dissipation of this energy has been incorporated into cross-shore hydrodynamics models by *Roelvink and Stive* [1989] and *Nairn et al.* [1990]. *Smith et al.* [1993] also embraced the TKE concept to explain a landward shift in the peak longshore current observed on barred beaches, a shift that could not be produced by tuning conventional mixing models.

In the study described herein, it is found that the transition region is governed not so much by a lag between turbulence production by breaking and dissipation in the wake left behind, but by a lag due to the time required to create the roller itself. This finding is in fact more akin to the original hypothesis of *Battjes and Janssen* [1978, p. 586], who postulated that “. . . in the breaking process S_{xx} [the radiation stress] decreases not as fast as the potential energy of the waves, perhaps due to a local relative surplus of kinetic energy of organized wave motions

¹Presently at the Conrad Blucher Institute for Surveying and Science, Texas A&M University-Corpus Christi.

and turbulent motions together." As will be seen, however, although the model developed in this study has the same basis as previous studies (an energy balance), there are crucial differences in the representation of the flux of TKE and in the choice of a dissipation function.

A final introductory point that motivates this investigation is that because of the difficulties encountered in hydrodynamic modeling in the transition region and because undertow plays a primary role in cross-shore transport [Dyhr-Nielsen and Sorensen, 1970; Dally and Dean, 1984; Roelvink and Stive, 1989], process-based sand transport and beach profile evolution models do not reliably predict the position and shape of the bar that forms near the breakpoint. Models capable of being driven by regular waves, i.e., Dally [1980], Dally and Dean [1984], and Hedegaard *et al.* [1991], exhibit discontinuities in flow and transport at the breakpoint, which must be smoothed in an ad hoc manner. Although much study has been devoted to measuring and modeling the vertical structure of undertow, in regard to beach evolution it appears to be more important to correctly represent the cross-shore structure of the cross-shore currents, especially in the transition region.

Roller Model Formulation

In general, past description of the roller has been limited to geometrical arguments and the use of semiempirical formulas to prescribe its cross-sectional area. On the basis of the measurements of Duncan [1981] of the steady breaking wave created behind a towed hydrofoil, Svendsen [1984b] assumed that the area of the roller, A , was given by

$$A = 0.9H^2 \quad (1)$$

in which H is the local wave height. Deigaard *et al.* [1991] assumed the roller was similar in size to the aerated region of a steady, fully developed hydraulic jump, and based on the work of Engelund [1981], modeled the area according to

$$A = (H^2/\tan \theta)[H/4(h + \bar{\eta})] \quad (2)$$

where θ is the angle of inclination of the boundary between the roller and the underlying organized flow ($\sim 10^\circ$), h is the local still water depth, and $\bar{\eta}$ is the mean water level. If applied in the outer surf zone, because of their dependence on wave height these models cause the strongest undertow to occur at the point of incipient breaking. In attempting to shift the peak in the undertow farther into the surf zone, Okayasu *et al.* [1986, 1988] adopted the model

$$A = \alpha\kappa HL \quad (3)$$

in which L is the local wave length and α and κ are empirically prescribed factors that depend upon position in the surf zone. The peak in undertow was shifted landward by increasing κ linearly from a value of zero at the breakpoint to a maximum value at the observed end of the transition region and then back to zero at the shoreline. This ad hoc treatment of the roller produced reasonable results for the observed cross-shore structure in mass flux, but required a priori knowledge of the extent of the transition region and involved several subjective measurements.

The present model for the roller area is more rigorously based on a depth-integrated (i.e., one-dimensional), time-averaged energy balance that contains contributions from both

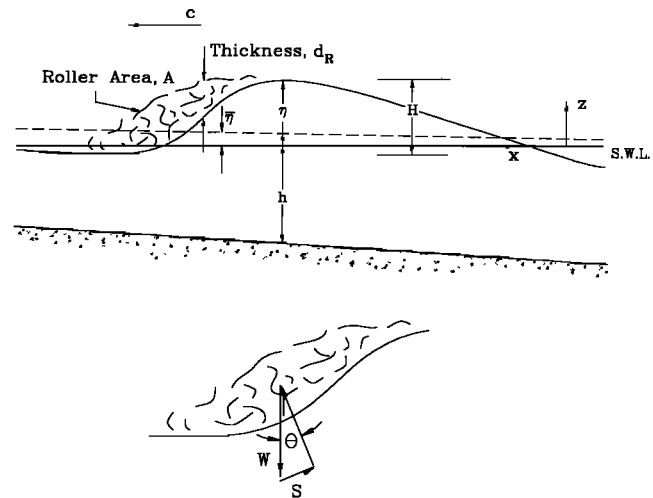


Figure 1. Definition sketch for roller model.

the organized wave motion and the roller, which can be expressed as

$$\frac{d\overline{F}_W}{dx} + \frac{d\overline{F}_R}{dx} = -\overline{D} \quad (4)$$

in which F_W is the energy flux (per unit length of crest) associated with the organized wave motion, F_R is the energy flux associated with the roller, and D is the rate of energy dissipation per unit planform area. The overbar denotes time averaging over one wave period, and x is directed onshore. This basic governing equation is essentially identical to that of Nairn *et al.* [1990]; however, different representations for both the energy flux in the roller and the dissipation will be adopted.

Referring to the definition sketch in Figure 1, the instantaneous flux of kinetic energy through a vertical section as the roller passes is given by

$$F_R = KE_R c d_R \quad (5)$$

where c is the wave celerity, d_R is the instantaneous thickness of the roller, and KE_R is the instantaneous kinetic energy density averaged over the roller thickness. In time averaging, these quantities can be represented as

$$\overline{KE}_R = \frac{1}{2} \rho_R (\beta_c c)^2 \quad (6)$$

$$\overline{d}_R = A/cT \quad (7)$$

where ρ_R is the average mass density in the aerated roller (assumed constant), and T is the wave period. It is noted that the cross-sectional area of the roller (A) includes entrained air. Although in establishing (6) it has been assumed that the average velocity in the roller is equal to the wave celerity [Svendsen, 1984a], the coefficient β_c is introduced as a means of accounting for the nonlinear dependence of the kinetic energy on the instantaneous water particle velocity. However, this coefficient is expected to be of order 1.0. The time-averaged energy flux associated with the roller becomes

$$\overline{F}_R = \frac{1}{2} \rho_R (\beta_c c)^2 \frac{A}{T} \quad (8)$$

In developing a dissipation function, Roelvink and Stive [1989] drew an analogy to the dissipation in a turbulent wake,

whereas *Svendsen* [1984a] and *Deigaard et al.* [1991] used that for a steady hydraulic jump. Here a dissipation term is adopted that is based on the assumption that the energy is dissipated at the interface between the turbulent roller and the underlying organized flow, an approach adopted and validated by *Duncan* [1981]. Referring once again to Figure 1, the weight of the roller per unit crest width (W) can be expressed as

$$W = \rho_R g A \quad (9)$$

and so for a force balance to exist, the shear between the roller and the underlying fluid is

$$S = W \sin \theta \quad (10)$$

By projecting this slightly inclined shear, which moves at the wave celerity, into the direction of roller motion, the time-averaged rate of energy dissipation per unit planform area is given by

$$\overline{D} = \frac{S \cos \theta c}{L} = \frac{\rho_R g A \sin \theta \cos \theta}{T} \quad (11)$$

Substituting (8) and (11) into (4) yields the governing equation for the creation and evolution of the roller area A :

$$\frac{d\overline{F}_w}{dx} + \frac{d}{dx} \left(\frac{1}{2} \rho_R \beta_c^2 c^2 \frac{A}{T} \right) = -\rho_R g \beta_D \frac{A}{T} \quad (12)$$

where β_D is a dissipation coefficient given by the angle of inclination of the roller ($\sin \theta \cos \theta$) and is the primary calibration coefficient for the model. Note that no attempt is made to relate the roller area to the local wave height (equations (1), (2), and (3)), which would be physically unrealistic in the growth phase of the roller.

In (12) it is also important to note that because the roller area invariably appears with the roller mass density (ρ_R) and wave period (T), the governing equation can be solved for the time-averaged mass flux of the roller ($\rho_R A/T$) explicitly. With T fixed, altering the value of ρ_R only serves to change A in a compensating manner, so that their product remains the same. This conveniently circumvents the problem of choosing a reliable value for the mass density of the aerated roller, which should be less than that of water.

Numerical Solution and Preliminary Findings

In seeking a solution to (12), wave celerity and a description of the gradient in organized wave energy flux are needed as input, as well as a single boundary condition. The obvious boundary condition is that $A = 0$ at the breakpoint. For driving the model, any one of several theories (e.g., Airy or stream function) could be used to parameterize the local organized energy flux in terms of wave height, mean water depth, and wave period, and then either measurements or a separate model used to provide the breaking height. In fact, if shallow water linear wave theory and the classic decay model $H \propto h$ are adopted, analytical solutions for the roller mass can be derived for monotonic beach profiles. For testing, calibrating, and verifying the roller model, however, a numerical solution will be employed. In addition, for driving the roller model, measured wave heights will be used in calculating \overline{F}_w , so that calibration will not be influenced by any shortcomings of a wave height decay model used to predict the cross-shore distribution of breaker height.

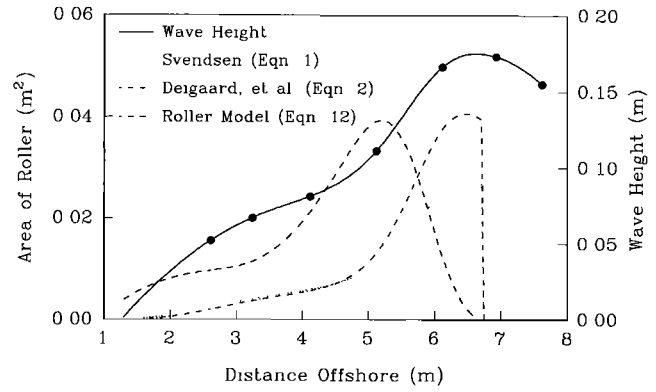


Figure 2. Roller area predicted by (12) in comparison with the models of *Svendsen* [1984a] and *Deigaard et al.* [1991] for test conditions of *Hansen and Svendsen* [1984]. Cubic splines were used to interpolate wave heights.

Assuming for the moment that \overline{F}_w and c are known (or that wave height and mean water level are known so that \overline{F}_w and c can be calculated from a wave theory), direct integration of (12) between grid point i and grid point $i + 1$ yields simply

$$\overline{F}_{w,i+1} - \overline{F}_{w,i} + \frac{\rho_R \beta_c^2}{2T} [(c^2 A)_{i+1} - (c^2 A)_i] = -\frac{\rho_R g \beta_D}{T} \int_{x_i}^{x_{i+1}} A \, dx \quad (13)$$

in which the integral is to be evaluated numerically. Because only one condition is available to start the solution ($A = 0$ at the breaker line), the trapezoid rule is employed, producing

$$\begin{aligned} \overline{F}_{w,i+1} - \overline{F}_{w,i} + \frac{\rho_R \beta_c^2}{2T} [(c^2 A)_{i+1} - (c^2 A)_i] \\ = -\frac{\rho_R g \beta_D \Delta x}{T} \left(\frac{A_{i+1} + A_i}{2} \right) \end{aligned} \quad (14)$$

which is accurate to second order in Δx and can be solved explicitly for A_{i+1} . A more accurate solution, e.g., using Simpson's rule or the corrected trapezoid rule, would require additional information. Figure 2 presents a comparison of this numerical solution ($\Delta x = 0.1$ m) to the roller models of *Svendsen* [1984a] and *Deigaard et al.* [1991]. Organized wave energy flux and celerity were calculated from linear theory, using the test conditions and measured wave heights and setup of *Hansen and Svendsen* [1984]. Cubic splines were used to provide wave height and setup information between measurement stations. This example was generated using a celerity coefficient (β_c) of 1.0 and a dissipation coefficient (β_D) of 0.10 ($\theta \sim 5.8^\circ$). Because aeration is neglected in both *Svendsen's* and *Deigaard et al.'s* models, the mass density in the roller was taken to be that of water to facilitate comparison.

For the new model the shift between the breakpoint and the location where the roller becomes fully developed is obvious. As will be shown, the evolution of the roller is responsible for moving the peak of the cross-shore current landward, as well as suppressing the initiation of setup. Figures 3 and 4 present the results of runs to test the sensitivity of the model to its celerity and dissipation coefficients, respectively. As was mentioned, the celerity coefficient β_c is expected to have a value near 1.0, and it is apparent from Figure 3 that varying the celerity coefficient across a realistic range of 0.8–1.2 does not move the

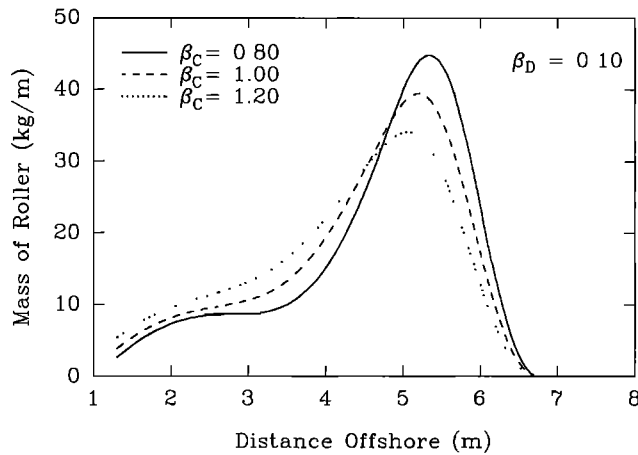


Figure 3. Sensitivity test of the roller model to the celerity coefficient (β_c) for experiment conditions of Hansen and Svendsen [1984].

peak in roller mass significantly but does somewhat alter the evolution of roller mass across the surf zone. On the other hand, Figure 4 displays a notable sensitivity of roller mass and its evolution to the dissipation coefficient, and so calibration of the model will focus on determining a reliable value for β_D . For reference, the measurements of Duncan [1981] of the angle of inclination of the aerated region for steady breakers produced by a towed hydrofoil are in the range of 10.0° – 14.7° , which corresponds to β_D in a range of 0.17–0.25.

Application to Cross-Shore Mean Hydrodynamics

If suitable input for the organized energy flux and wave celerity were available, the roller model could be used autonomously. However, owing to a lack of suitable roller measurements, calibration of the model requires that roller terms first be incorporated into the cross-shore mean mass balance and then suitable values for β_D and β_c be chosen based on comparison to observed undertow. Calculation of the depth-averaged undertow velocity in turn requires local setup information in order to establish the total mean water depth.

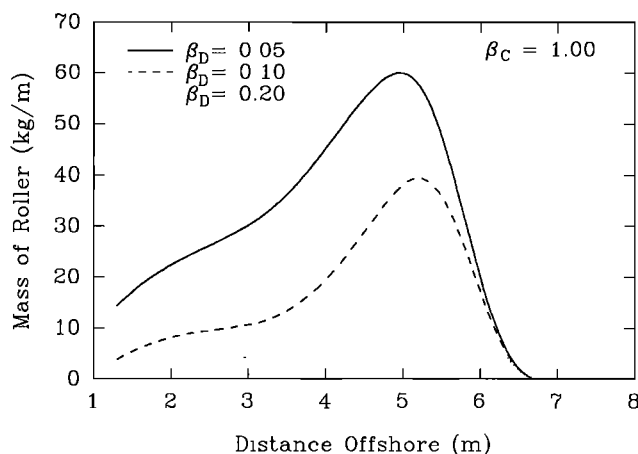


Figure 4. Sensitivity test of the roller model to the dissipation coefficient (β_D) for experiment conditions of Hansen and Svendsen [1984].

Because setup measurements are not provided with several of the data sets to be examined, the mean cross-shore momentum balance must also be included in the model. It can be argued, however, that this approach to calibration and verification is more meaningful anyway, because accurate prediction of mean currents and setup is a primary goal in practical surf zone modeling.

With a shoreline present the onshore water volume flux that takes place above the mean water level (mwl) due to the wave motion must be locally balanced by the offshore discharge below mwl due to the cross-shore current [Dally, 1980]. This is of course founded upon the vertically integrated, time-averaged continuity equation

$$\frac{d}{dx} [U(h + \bar{\eta})] + \frac{dQ_w}{dx} + \frac{dQ_R}{dx} = 0 \quad (15)$$

in which U is the depth-averaged (below mwl) current, Q_w is the volume flux per unit crest width associated with the organized wave motion, and Q_R is the fluid volume flux due to the roller ($\rho_R A / \rho T$).

The vertically integrated, time-averaged cross-shore momentum balance is given by

$$\rho g(h + \bar{\eta}) \frac{d\bar{\eta}}{dx} + \frac{dS_{xx}}{dx} - \frac{d}{dx} [\rho U^2(h + \bar{\eta})] + \frac{dM_R}{dx} = -\bar{\tau}_b \quad (16)$$

in which S_{xx} is the radiation stress associated with the organized wave motion [Longuet-Higgins and Stewart, 1964], M_R is the momentum flux due to the roller (calculated as $\rho_R \beta_c c A / T$), and $\bar{\tau}_b$ is the time-averaged bed stress. The third term on the left-hand side is the convective acceleration of the current. Although this term has been neglected in previous investigations, it will be shown here to be larger than the bed stress. It is also noted that in deriving (16), the influence of the vertical structure of the undertow on the force balance has been neglected. This can be justified in the surf zone, where the undertow measurements of Nadaoka and Kondoh [1982] show the current to be almost uniform with depth. Outside the breakpoint, however, vertical structure is more evident in their measurements (see also Putrevu and Svendsen [1993]). A rigorous derivation and discussion of (15) and (16) are provided by Dally [1995]; see also Brown [1993].

The bed stress is modeled according to the quadratic friction model given by

$$\bar{\tau}_b = \rho(f/8)\overline{u_b|u_b|} \quad (17)$$

where f is a Darcy-Weisbach friction factor and u_b is the total instantaneous velocity (oscillatory plus mean) near the bed. Assuming sinusoidal oscillatory motion and assuming the mean current is small, it can be shown that (17) reduces to

$$\bar{\tau}_b = (\rho f / 2\pi) \hat{u}_m U \quad (18)$$

where \hat{u}_m is the maximum wave oscillatory velocity near the bed, taken herein from linear theory [see LeBlond and Tang, 1974].

Following Smith et al. [1993], by equating the Manning formula and the Darcy-Weisbach equation, the friction factor can be expressed as

$$f = 8gn^2/(h + \bar{\eta})^{1/3} \quad (19)$$

where n is the Manning resistance coefficient. In developing (19), it has been assumed that the hydraulic radius is equal to

the local water depth. Manning's coefficient has dimensions of [time/length^{1/3}], and a value of 0.019 s m^{-1/3} is adopted.

Applying the boundary condition that there is no mean flow at the shoreline, (15) is integrated, which yields

$$U_{i+1} = -(Q_W + Q_R)_{i+1}/(h + \bar{\eta})_{i+1} \quad (20)$$

Before integrating (16), it is first noted that

$$(h + \bar{\eta}) \frac{d\bar{\eta}}{dx} = \frac{1}{2} \frac{d}{dx} (h + \bar{\eta})^2 - (h + \bar{\eta}) \frac{dh}{dx}$$

and integrating produces

$$\begin{aligned} & \frac{\rho g}{2} [(h + \bar{\eta})_{i+1}^2 - (h + \bar{\eta})_i^2] - \rho g \int_{x_i}^{x_{i+1}} \left[(h + \bar{\eta}) \frac{dh}{dx} \right] dx \\ & + (S_{xx_{i+1}} - S_{xx_i}) + (M_{R_{i+1}} - M_{R_i}) - \rho([U^2(h + \bar{\eta})]_{i+1} \\ & - [U^2(h + \bar{\eta})]_i) = -\frac{\rho}{2\pi} \int_{x_i}^{x_{i+1}} (f\hat{u}_m U) dx \quad (21) \end{aligned}$$

Again using the trapezoid rule to evaluate the integrals

$$\begin{aligned} & \frac{\rho g}{2} [(h + \bar{\eta})_{i+1}^2 - (h + \bar{\eta})_i^2] \\ & - \rho g \Delta x \left(\frac{[(h + \bar{\eta})(-m)]_{i+1} + [(h + \bar{\eta})(-m)]_i}{2} \right) \\ & + (S_{xx_{i+1}} - S_{xx_i}) + (M_{R_{i+1}} - M_{R_i}) - \rho([U^2(h + \bar{\eta})]_{i+1} \\ & + [U^2(h + \bar{\eta})]_i) = -\frac{\rho \Delta x}{2\pi} \left[\frac{(f\hat{u}_m U)_{i+1} + (f\hat{u}_m U)_i}{2} \right] \quad (22) \end{aligned}$$

in which m is the local bottom slope. Expecting the bottom profile, still water level, wave period, setup at the outermost grid point, and $H(x)$ to be provided, the system of three equations, (14), (20), and (22), is solved for the three unknowns ($\rho_R A$), $(h + \bar{\eta})$, and U in the following manner. Moving stepwise across the transect, a first estimate of $(\rho_R A)_{i+1}$ is calculated from (14), using the setup from the previous grid point. The cross-shore current U_{i+1} is then estimated from (20) and inserted into (22), and $(h + \bar{\eta})_{i+1}$ calculated by applying the quadratic formula, always selecting the positive root. With the refined value for $\bar{\eta}_{i+1}$, the integral properties and $(\rho_R A)_{i+1}$ are recalculated and the procedure iterated. It is noted that if the model is started outside the surf zone, creation of the roller does not begin, intrinsically, until there is a decrease in the calculated organized energy flux used in (14).

In all of the calibration and verification runs to be discussed below, a convergence criterion of 0.1% change in $(h + \bar{\eta})$ was employed. With a grid spacing of 0.1 m, no more than three iterations were required at any grid point. If setup measurements were provided, the vertical datum was set at the mwl at the outermost measurement station, i.e., $\bar{\eta}_1 = 0$. The solution progressed from offshore to onshore and was stopped when the mean water depth became less than 0.01 m.

In order to calculate wave celerity and the energy, mass, and momentum flux terms associated with the organized, oscillatory wave motion, a nonbreaking wave theory must be adopted. As a baseline, the well-known expressions for these quantities

provided by linear wave theory can be utilized [see *Dean and Dalrymple*, 1984]. As might be expected, however, it was found that use of a nonlinear theory, specifically stream function theory [Dean, 1974], denoted SFT, greatly improved the predictive capabilities of the roller/undertow models. The integral properties required by the model are tabulated by *Dean* [1974] in dimensionless form for discrete wave steepnesses and relative depths. A cubic spline algorithm was once again used to interpolate for the specific conditions at each point on the transect.

Calibration

The roller model was calibrated using the laboratory data for undertow reported by *Hansen and Svendsen* [1984]. This set was chosen for calibration because (1) the waves in this experiment were of the spilling breaker type, for which the formulation of the roller model would seem most appropriate, and (2) the bottom slope was in the middle of the range of all of the laboratory studies available in the literature. In this two-dimensional wave channel study, vertical profiles of mean cross-shore currents were determined by time averaging the measurements of micropropeller current meters, taken at 5–7 elevations below the wave trough level. The profiles were measured at five stations on a planar beach of 1/34.25 slope, for regular wave conditions with a period of 2.0 s and a breaker height of 0.17 m. Four of the measurement stations were inside the breakpoint. Depth-averaged currents, determined by numerical integration of the observed profiles, as well as mean water level elevations, are also reported by *Svendsen et al.* [1987].

In general, global values for the dissipation and celerity coefficients of the roller model were chosen such that the best representation (by eye) of the cross-shore distribution of depth-averaged undertow was obtained for the *Hansen and Svendsen* [1984] data set. Figure 5 presents comparisons of model output to the data, generated using both linear wave theory and SFT for the integral properties associated with the organized motion. Setting the celerity coefficient at its most obvious value ($\beta_c = 1.0$) and using SFT, the value for the dissipation coefficient that produced a very good comparison to the undertow was $\beta_D = 0.10$. For linear wave theory the coefficients of the roller model could not be tuned (using realistic values) to produce a comparison that was even marginally comparable to that for SFT. This is attributed to an overestimation of the mean mass transport associated with the organized wave motion, i.e., the Stokes drift. This is particularly evident in Figure 5a before breaking is initiated. The results of sensitivity tests for β_c and β_D , using SFT, are displayed in Figures 6 and 7. From these tests it can be concluded that (1) there is no compelling reason to adopt a celerity coefficient different from 1.0 and (2) with a uniform dissipation coefficient of 0.10, the roller model yields very good estimates of both undertow and setup across the entire surf zone for this data set.

Verification

With the roller model calibrated in terms of cross-shore currents with the undertow data of *Hansen and Svendsen* [1984], independent verification can be attempted using other appropriate laboratory data that are available in the literature.

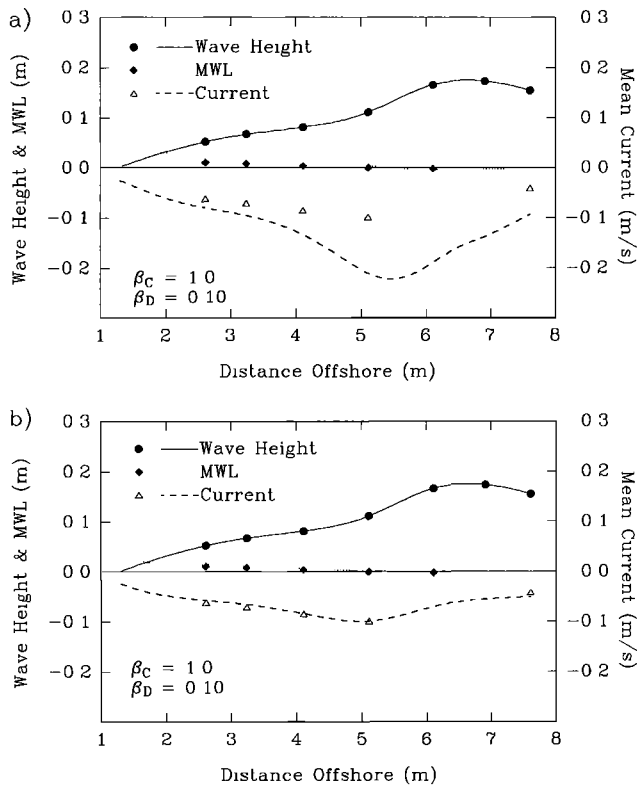


Figure 5. Depth-averaged (below mean water level) currents and setup predicted by model (equations (12), (15), and (16)), with integral properties calculated using (a) linear wave theory and (b) stream function theory, in comparison with measurements of *Hansen and Svendsen* [1984].

These data sets and their associated test conditions are listed in Table 1, along with that for the *Hansen and Svendsen* [1984] investigation. All studies were conducted for regular waves breaking on planar beach profiles. Bottom slope ranged from 1/20 to 1/40, wave steepness at the breakpoint ranged from 0.016 to 0.077, and breaker types included both spilling and plunging. The results of all of these experiments were reported as vertical profiles of the mean cross-shore current, measured at different locations along the wave channel, and so values for depth-averaged currents were determined by digitizing and numerically integrating the reported undertow profiles. Using wave heights splined between measured values, model predictions using both linear and stream function theories are presented in comparison to these data for undertow and setup (if reported) in Figures 8–12.

The comparisons of the roller/currents model to these data sets are encouraging. In particular, if SFT is used instead of linear theory to describe the organized motion, the predictions are notably improved, especially for the low-steepness conditions. In all comparisons the shift between the breakpoint and the point of maximum current is faithfully reproduced. Also, for those experiments where mean water levels were reported, the delay in the initiation of setup is well represented.

To make an objective, quantitative assessment of the validity of the roller/currents model, root-mean-square (rms) error can be calculated for the predicted undertow and is defined by

$$\epsilon = \left[\frac{\sum (U_{\text{meas}} - U_{\text{model}})^2}{\sum U_{\text{meas}}^2} \right]^{1/2} \quad (23)$$

The rms errors calculated for all six data sets are presented in Table 2. Average error is less than 19%.

Although it appears that reliable results can be obtained if SFT is used in computing the integral properties of the organized motion that are required by the models, SFT does assume steady, symmetric waves, which is certainly not the case near and in the surf zone. These assumptions are violated most in the shoaling region near the point of incipient breaking and before the roller is developed. However, Figures 8–12 show that SFT predicts the mean mass flux near the breakpoint quite well, and similar results should be expected for the other averaged properties required by the model (celerity, energy flux, and momentum flux). In addition, because a theory is required to provide the period-averaged energy flux for the organized motion, not only is direct verification of the roller formulation impossible, but also any inaccuracy in the theory affects the calibration, i.e., the choice of the value for the dissipation coefficient. However, the fact that the SFT-driven hydrodynamics model works well (1) across the entire surf zone, (2) for a wide range of test conditions, and (3) with essentially one empirical coefficient fixed at a universal value ($\beta_D = 0.10$) lends credibility to the specific formulations for the roller energy flux (equation (8)) and dissipation (equation (11)).

Finally, a time-dependent wave model might be utilized for representing the organized motion, such as the Boussinesq-based model of *Schäffer et al.* [1993]. However, time-dependent models are already CPU-intensive, and coupled with the added

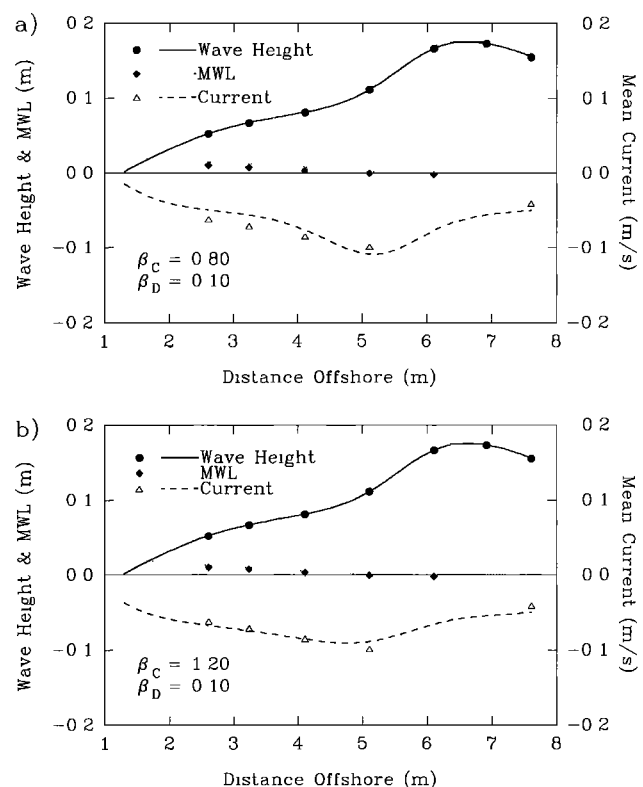


Figure 6. Results of sensitivity tests using celerity coefficients (β_C) of (a) 0.80 and (b) 1.20, in comparison with measurements of *Hansen and Svendsen* [1984].

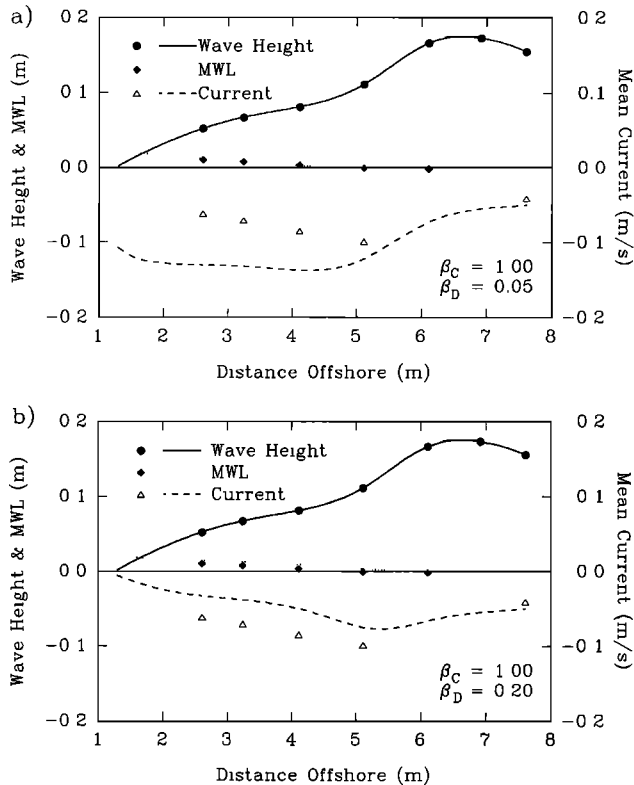


Figure 7. Results of sensitivity tests using dissipation coefficients (β_D) of (a) 0.05 and (b) 0.20, in comparison with measurements of *Hansen and Svendsen* [1984].

burden of computing averages for the bed stress and mass, momentum, and energy fluxes, any improvement realized would be costly. This is unwarranted in the present context, especially with SFT already providing acceptable results.

Discussion

In the course of this modeling investigation it was confirmed that in order to accurately depict the cross-shore distribution of cross-shore currents, it is necessary to use the roller model and stream function theory in concert; i.e., relatively sophisticated treatments of both the organized motion and the turbulent roller are required. Although linear theory works remarkably well in the inner surf zone, the importance of using a nonlinear wave theory in the outer surf zone is clearly evident in Figures 5 and 8–12. This is especially true for low-steepness waves, as should be expected.

The merit of the roller model (equation (12)) is attributed to the fact that the size of the roller has not been parameterized

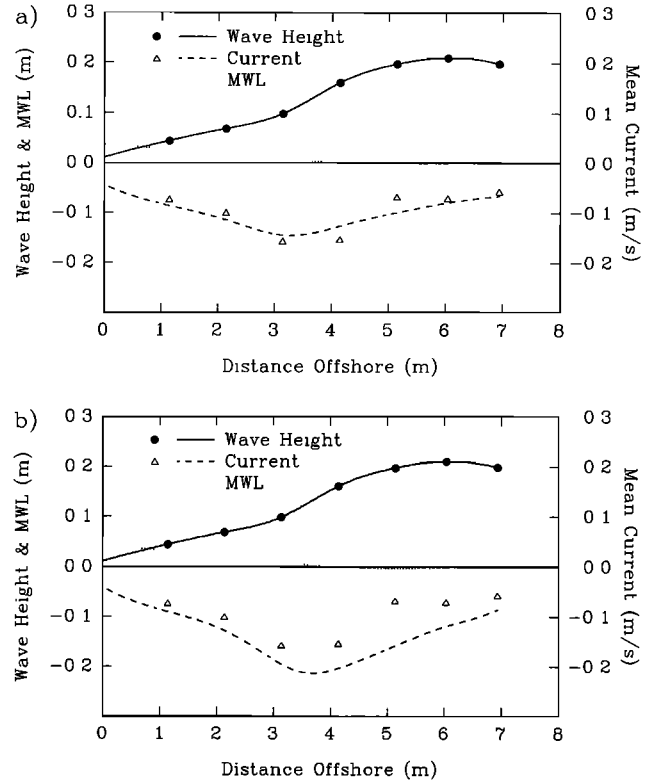


Figure 8. Comparison of model to measurements of *Nadaoka and Kondoh* [1982, case 1], using (a) stream function theory and (b) linear wave theory to calculate integral properties of the organized wave motion.

in terms of the local wave height, as is the case with (1), (2), and (3), but is allowed to grow and evolve as dictated by gradients in the organized energy flux. Adopting the roller as the key component of the energy balance, as opposed to the turbulent wake left behind, is also essential. The particular representation chosen for the flux of energy in the roller, and especially the form adopted for the energy dissipation, depart significantly from those adopted in the earlier TKE/turbulent wake approach of *Roelvink and Stive* [1989] and *Smith et al.* [1993]. For example, when cast in notation consistent with (12), the *Roelvink and Stive* [1989] turbulent wake-based model is given by

$$\frac{d\overline{F}_w}{dx} + \frac{d}{dx} [\rho\alpha_f \bar{k} c (h + \bar{\eta})] = -\rho\alpha_D \bar{k}^{3/2} \quad (24)$$

in which \bar{k} is the average TKE per unit mass, and α_f and α_D are coefficients argued to be approximately 1.0. In developing the TKE balance, a length scale for the turbulence and a

Table 1. Summary of Data Sets Used for Calibration and Verification of the Roller Model

Data Set	Bottom Slope	H_b , m	Period, s	H_b/L_o	Breaker Type
<i>Hansen and Svendsen</i> [1984]*	1/34	0.17	2.00	0.0277	spilling
<i>Nadaoka and Kondoh</i> [1982, case 1]	1/20	0.21	1.32	0.0772	spilling
<i>Nadaoka and Kondoh</i> [1982, case 5]	1/20	0.25	2.34	0.0291	plunging
<i>Okayasu et al.</i> [1988, case 2]	1/20	0.10	2.00	0.0162	plunging
<i>Okayasu et al.</i> [1986, case 3]	1/20	0.12	1.50	0.0339	plunging
<i>Stive and Wind</i> [1986, case 1]	1/40	0.18	1.79	0.0356	spilling

*Only set used in calibration.

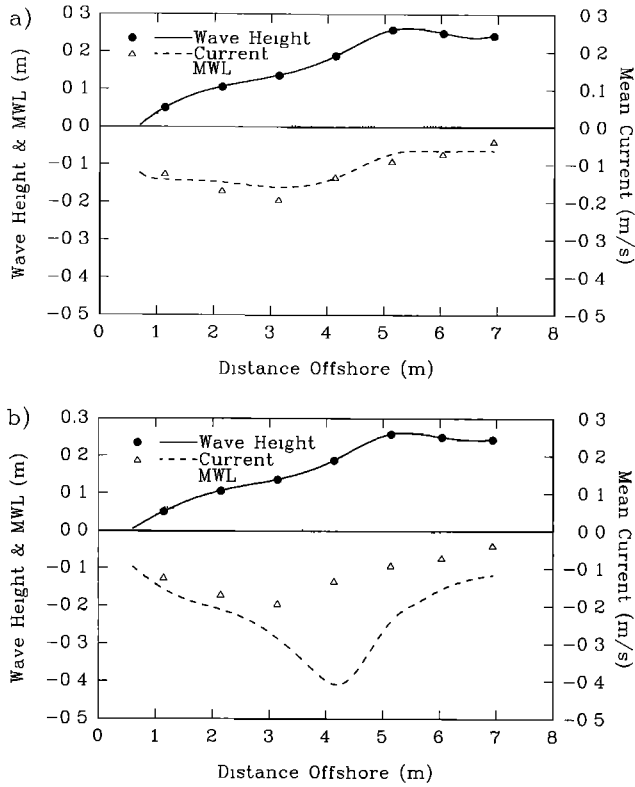


Figure 9. Comparison of model with measurements of *Nadaoka and Kondoh* [1982, case 5], using (a) stream function theory and (b) linear wave theory to calculate integral properties of the organized wave motion.

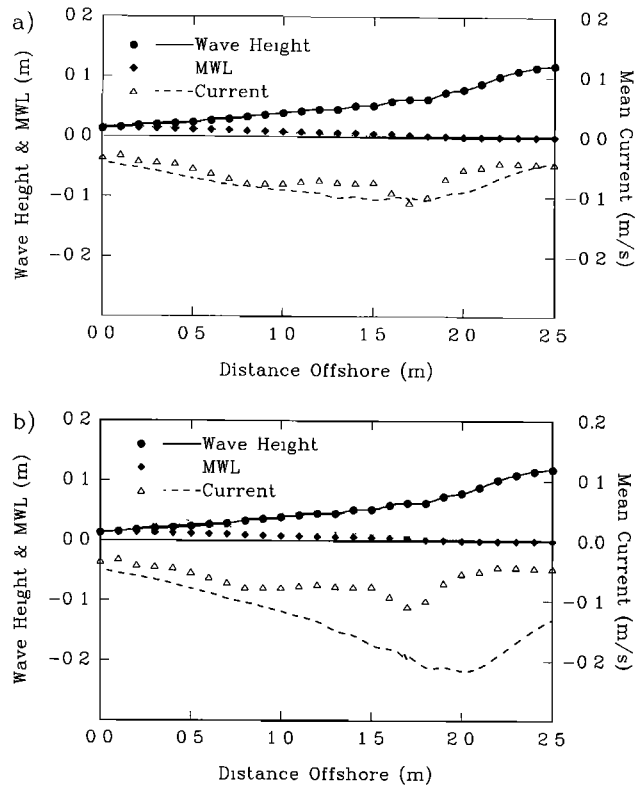


Figure 11. Comparison of model with measurements of *Okayasu et al.* [1986, case 3], using (a) stream function theory and (b) linear wave theory to calculate integral properties of the organized wave motion.

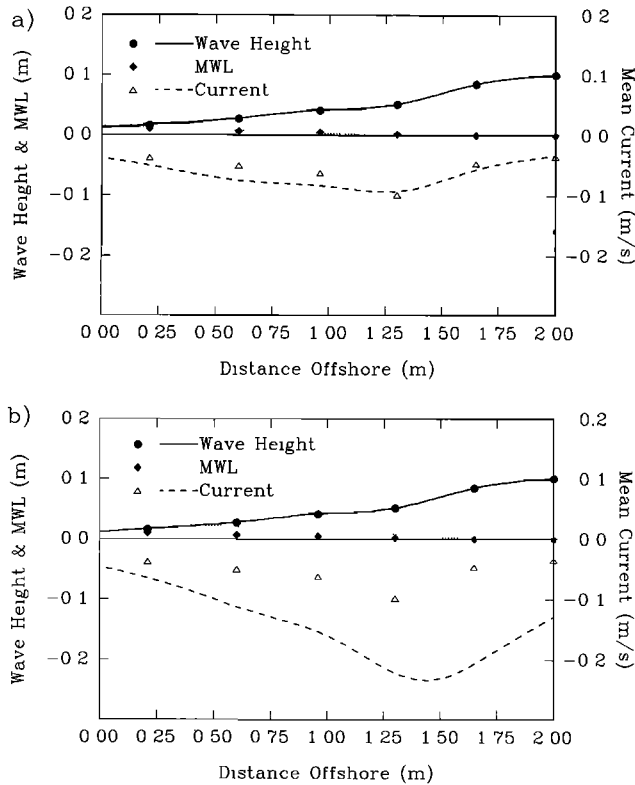


Figure 10. Comparison of model with measurements of *Okayasu et al.* [1988, case 2], using (a) stream function theory and (b) linear wave theory to calculate integral properties of the organized wave motion.

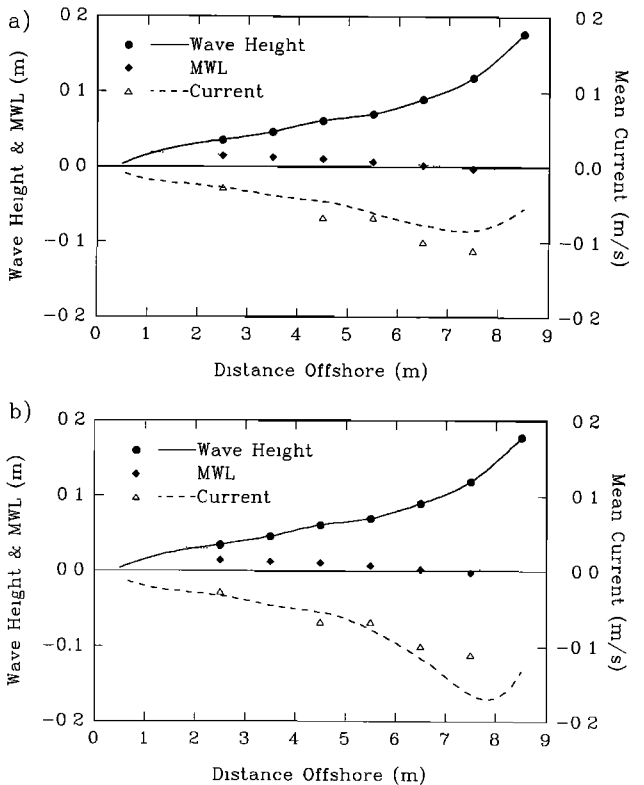


Figure 12. Comparison of model with measurements of *Stive and Wind* [1986], using (a) stream function theory and (b) linear wave theory to calculate integral properties of the organized wave motion.

Table 2. Root-Mean-Square Error for Predicted Depth-Averaged Current, Using Stream Function and Linear Wave Theories in Calculating Integral Properties

Data Set	Stream Function	Linear
<i>Hansen and Svendsen</i> [1984]	7	82
<i>Nadaoka and Kondoh</i> [1982, case 1]	17	48
<i>Nadaoka and Kondoh</i> [1982, case 5]	16	103
<i>Okayasu et al.</i> [1988, case 2]	24	187
<i>Okayasu et al.</i> [1986, case 3]	25	134
<i>Stive and Wind</i> [1986, case 1]	23	31

Values are in percent.

penetration depth have also been estimated. Representing the momentum flux associated with the TKE as $M_{\text{wake}} = 0.22\rho\bar{k}(h + \bar{\eta})$, as recommended by Roelvink and Stive, and the associated volume flux as $Q_{\text{wake}} = M_{\text{wake}}/\rho c$, the system of (24), (15), and (16) can be solved as before. The results are shown in Figure 13 in comparison to the *Hansen and Svendsen* [1984] data and are clearly not as favorable as for the roller model.

Of course, breaking waves dissipate energy not only at the roller interface but also in both the body of the roller and in the wake left behind; however, Figure 13 demonstrates that the dissipation in the turbulent wake has little effect on the mass and momentum balances. Tests with the TKE model also show that in order to obtain reasonable predictions of mass flux and setup, its coefficients must be set at values roughly 8 times greater than are realistic. This finding indicates that in the mean balances of energy, momentum, and mass, the impor-

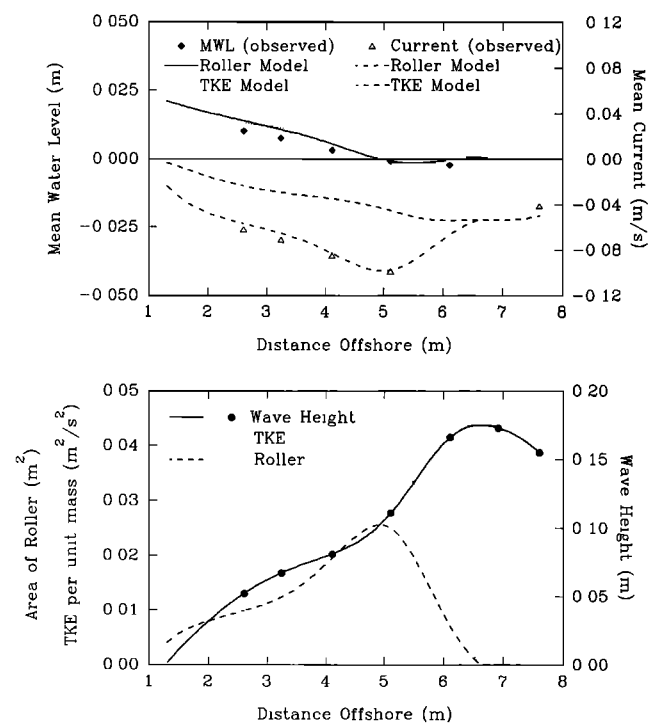


Figure 13. Comparison of turbulent wake-based model of Roelvink and Stive [1989] (equation (24)) with the data of *Hansen and Svendsen* [1984] and the roller model. Upper panel presents setup and undertow results. Lower panel presents observed wave height, modeled roller area, and turbulent kinetic energy.

tance of the turbulent wake left behind is small compared to that of the roller itself. In addition, although it is difficult to directly assess the dissipation in the body of the roller, the results of the model's verification substantiate the claim that the dissipation at the interface dominates; otherwise, β_D would have to be set at an unrealistically high value.

The importance of the roller in correctly predicting the mean cross-shore hydrodynamics is highlighted by Figure 14, which shows the setup and undertow generated with the roller terms neglected (but SFT retained) for the conditions of *Hansen and Svendsen* [1984] and *Nadaoka and Kondoh* [1982, case 1]. Without the roller the strength and distribution of both the undertow and setup are poorly represented. This figure also adds support to the conclusion once again that SFT adequately provides the mean mass flux in the zone of incipient breaking.

Figure 15 contrasts the mass flux associated with the roller ($\rho_R A/T$) with that due to the organized wave motion (Stokes drift) calculated from SFT for the *Hansen and Svendsen* [1984] case. This comparison confirms that once the roller becomes fully developed, its mass flux is comparable to or greater than that due to the organized motion, as was argued by *Svendsen* [1984b].

Figure 16 displays the cross-shore behavior of the terms in the momentum balance (equation (16)), with each gradient calculated using a central difference. The roller momentum flux, radiation stress, and setup-induced pressure gradient terms are clearly the most important. Interestingly, the convective acceleration term, which has been neglected in previous studies, appears to be more important than the bed stress. In fact, it appears that the bed stress is essentially negligible in the cross-shore mean momentum balance.

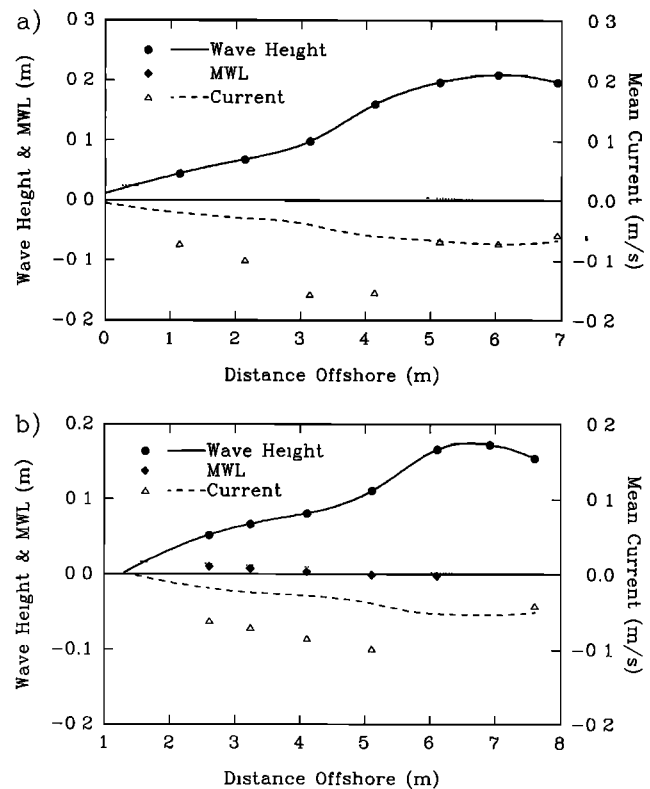


Figure 14. Model results computed using stream function theory, but with the roller neglected, in comparison with the data of (a) *Nadaoka and Kondoh* [1982, case 1] and (b) *Hansen and Svendsen* [1984].

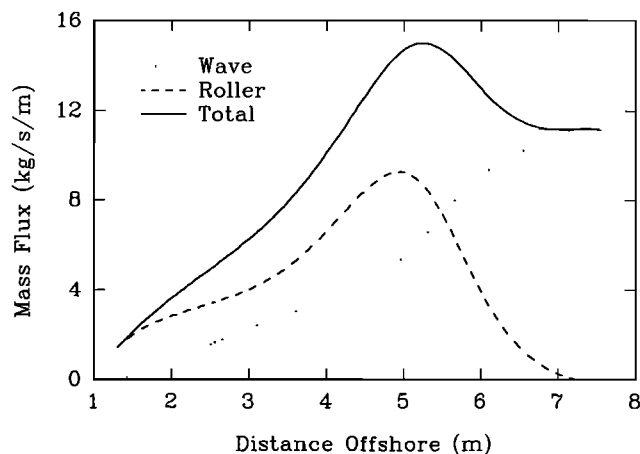


Figure 15. Comparison of the mass flux due to organized wave motion (from stream function theory) with the mass flux due to surface roller, for the experiment conditions of Hansen and Svendsen [1984].

Conclusions

By applying the model developed herein for the creation and evolution of the aerated roller associated with wave breaking and by utilizing stream function wave theory to provide integral properties for the organized wave motion, mean cross-shore hydrodynamics can be more faithfully represented in the nearshore. In particular, depth-averaged cross-shore currents and set-down and setup in the transition region and outer surf zone can now be modeled successfully for regular waves breaking on simple bottom profiles. The key features of the modeling are that (1) the size of the roller evolves in response to the

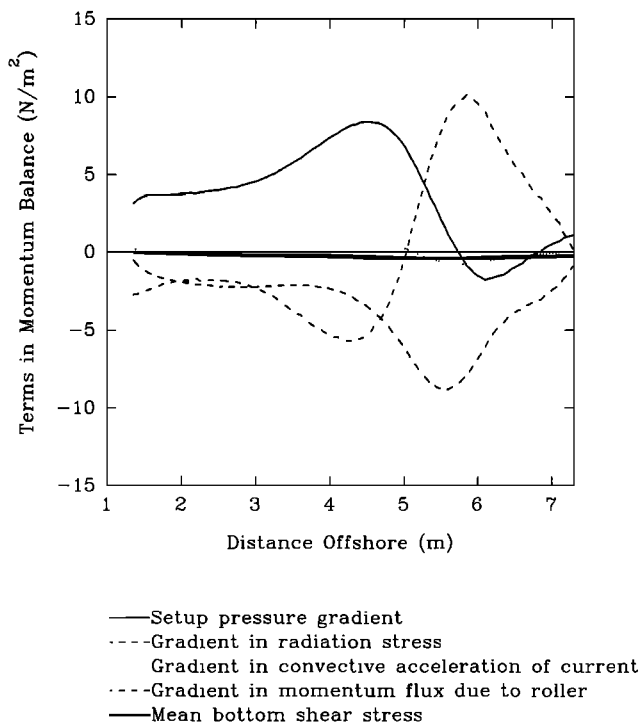


Figure 16. Comparison of terms in the momentum balance (equation (16)) for the experiment conditions of Hansen and Svendsen [1984].

gradient in organized energy flux and is not parameterized in terms of local wave height and (2) the roller itself, as opposed to its turbulent wake, is modeled as a major contributor to the energy, mass, and momentum balances. The empirical dissipation coefficient contained in the roller model has a nominal value of $\beta_D \approx 0.10$.

On the basis of the model results presented, the mean bed stress is negligible in the depth-integrated, cross-shore balance of momentum. However, in anticipation of applying the roller model to longshore mean hydrodynamics, bed stress is expected to remain important in the momentum balance in order to retard the longshore current.

It is noted that the roller and current models are fully applicable to more complex profile shapes, including bar/trough formations. They also can be directly extended to random waves, for example, by suitably averaging the energy, mass, and momentum flux terms for the organized wave motion.

Finally, with a process-based sediment transport and profile evolution model formulated for random waves, Roelvink and Stive [1989] have already demonstrated that predictions of bar position and shape can be improved if the observed landward shift of the peak in undertow is better represented. Random waves, however, do fortuitously "presmooth" the forcing and transport rates in the outer surf zone, thereby obscuring some of the details of interest in the transition region (where the bar usually forms). With the new roller model these details, which are accentuated in regular wave experiments, might soon be faithfully modeled.

Acknowledgments. This article was developed under the auspices of the Florida Sea Grant College Program with support from the National Oceanic and Atmospheric Administration, Office of Sea Grant, U.S. Department of Commerce, grant NA89AA-D-SG053.

References

- Battjes, J. A., and J. P. F. M. Janssen, Energy loss and set-up due to breaking in random waves, *Proc. Coastal Eng. Conf.*, 16, 569-587, 1978.
- Borekci, O. S., Distribution of wave-induced momentum fluxes over depth and application within the surf-zone, Ph.D. dissertation, Dep. of Civil Eng., Univ. of Del., Newark, 1982.
- Bowen, A. J., D. L. Inman, and V. P. Simmons, Wave "set-down" and set-up, *J. Geophys. Res.*, 73(8), 2569-2577, 1968.
- Brown, C. A., Modelling of cross-shore currents in the surf zone, M.S. thesis, Dep. of Oceanogr., Ocean Eng., and Environ. Sci., Fla. Inst. of Technol., Melbourne, 1993.
- Dally, W. R., A numerical model for beach profile evolution, M.S. thesis, Dep. of Civil Eng., Univ. of Del., Newark, 1980.
- Dally, W. R., Development of governing equations for wave, wind, and tide-driven currents for numerical modeling of the Sebastian Inlet system, report to the Sebastian Inlet Tax District Commission, 33 pp., Indianalantic, Fla., 1995.
- Dally, W. R., and R. G. Dean, Suspended sediment transport and beach profile evolution, *J. Waterw. Port Coastal Ocean Div. Am. Soc. Civ. Eng.*, 110(1), 15-33, 1984.
- Dean, R. G., Evaluation and development of water wave theories for engineering applications, *Spec. Rep. 1*, U.S. Army Waterw. Exp. Stn., Vicksburg, Miss., 1974.
- Dean, R. G., and R. A. Dalrymple, *Water Wave Mechanics for Engineers and Scientists*, Prentice-Hall, Englewood Cliffs, N. J., 1984.
- Deigaard, R., P. Justesen, and J. Fredsøe, Modeling of undertow by a one-equation turbulence model, *Coastal Eng.*, 15, 431-458, 1991.
- Duncan, J. H., An experimental investigation of breaking waves produced by a towed hydrofoil, *Proc. R. Soc. London A*, 377, 331-348, 1981.
- Dyhr-Nielsen, M., and T. Sorensen, Some sand transport phenomena on coasts with bars, *Proc. Coastal Eng. Conf.*, 12, 855-865, 1970.
- Engelund, F., A simple theory of weak hydraulic jumps, in *Prog. Rep.*

- 54, pp. 29–32, Inst. of Hydrodyn. and Hydraul. Eng. (ISVA), Tech. Univ. of Denmark, Horsholm, 1981.
- Hansen, J. B., and I. A. Svendsen, A theoretical and experimental study of undertow, *Proc. Coastal Eng. Conf.*, 19, 2246–2262, 1984.
- Hedegaard, I. A., R. Deigaard, and J. Fredsøe, Onshore/offshore sediment transport and morphological modeling of coastal profiles, in *Proceedings of Coastal Sediments '91*, pp. 643–657, Am. Soc. of Civ. Eng., New York, 1991.
- LeBlond, P. H., and C. L. Tang, On energy coupling between waves and rip currents, *J. Geophys. Res.*, 79(6), 811–816, 1974.
- Longuet-Higgins, M. S., and R. W. Stewart, Radiation stresses in water waves: A physical discussion, with applications, *Deep Sea Res.*, 11, 529–562, 1964.
- Nadaoka, K., and T. Kondoh, Laboratory measurements of velocity field structure in the surf zone by LDV, *Coastal Eng. Jpn.*, 25, 125–145, 1982.
- Nairn, R. B., J. A. Roelvink, and H. N. Southgate, Transition zone width and implications for modeling surf zone hydrodynamics, *Proc. Coastal Eng. Conf.*, 22, 68–81, 1990.
- Okayasu, A., T. Shibayama, and N. Mimura, Velocity field under plunging waves, *Proc. Coastal Eng. Conf.*, 20, 660–674, 1986.
- Okayasu, A., T. Shibayama, and N. Mimura, Vertical variation of undertow in the surf zone, *Proc. Coastal Eng. Conf.*, 21, 478–491, 1988.
- Putrevu, U., and I. A. Svendsen, Vertical structure of the undertow outside the surf zone, *J. Geophys. Res.*, 98(C12), 22,707–22,716, 1993.
- Roelvink, J. A., and M. J. F. Stive, Bar-generating cross-shore flow mechanisms on a beach, *J. Geophys. Res.*, 94(C4), 4785–4800, 1989.
- Schäffer, H. A., P. A. Madsen, and R. Deigaard, A Boussinesq model for waves breaking in shallow water, *Coastal Eng.*, 20, 185–202, 1993.
- Smith, J. M., M. Larson, and N. C. Kraus, Longshore current on a barred beach: Field measurements and calculation, *J. Geophys. Res.*, 98(C12), 22,717–22,731, 1993.
- Stive, M. J. F., and H. G. Wind, Cross-shore mean flow in the surf zone, *Coastal Eng.*, 10, 325–340, 1986.
- Svendsen, I. A., Wave heights and set-up in a surf zone, *Coastal Eng.*, 8, 303–329, 1984a.
- Svendsen, I. A., Mass flux and undertow in a surf zone, *Coastal Eng.*, 8, 347–365, 1984b.
- Svendsen, I. A., H. A. Schäffer, and J. B. Hansen, The interaction between the undertow and the boundary layer flow on a beach, *J. Geophys. Res.*, 92(C11), 11,845–11,856, 1987.
-
- C. A. Brown, Conrad Blucher Institute for Surveying and Science, Texas A&M University-Corpus Christi, 6300 Ocean Drive, Corpus Christi, TX 78412. (e-mail: cbrown@cbi.tamucc.edu)
- W. R. Dally, Ocean Engineering Program, Florida Institute of Technology, 150 W. University Boulevard, Melbourne, FL 32901. (e-mail: wdally@winnie.fit.edu)

(Received March 30, 1994; revised July 6, 1995;
accepted August 20, 1995.)